



Arsenic mobility in alteration products of sulfide-rich, arsenopyrite-bearing mine wastes, Snow Lake, Manitoba, Canada

Kristin A. Salzsauler ^{*}, Nikolay V. Sidenko, Barbara L. Sherriff

Department of Geological Sciences, University of Manitoba, Winnipeg, Man., Canada R3T 2N2

Received 15 November 2004; accepted 9 June 2005

Editorial handling by R. Wanty

Available online 21 October 2005

Abstract

The Arsenopyrite Residue Stockpile (ARS) in Snow Lake, Manitoba contains approximately 250,000 tons of cyanide treated, refractory arsenopyrite ore concentrate. The residue was deposited between 1950 and 1959 in an open waste rock impoundment, and remained exposed until 2000, when the pile was capped with layers of waste rock and clay. During the time when the ARS was exposed to the atmosphere, arsenopyrite, pyrrhotite, pyrite and chalcopyrite were oxidized producing scorodite, jarosite and two generations of amorphous Fe sulfo-arsenates (AISA). These secondary phases attenuated some of the As released to pore water during oxidation in the upper layers of the ARS. The imposition of the cap prevented further oxidation. The secondary As minerals are not stable in the reduced environment that currently dominates the pile. Therefore, As currently is being released into the groundwater. Water in an adjacent monitoring well has concentrations of >20 mg/L total As with relative predominance of As(III).

© 2005 Elsevier Ltd. All rights reserved.

1. Introduction

Mining and beneficiation of ore deposits, where Au is associated with arsenopyrite and sulfides, produces As-rich mine wastes. Oxidation of sulfides can result in the mobilization and migration of As from these wastes into the environment (Leblanc et al., 1996; Roussel et al., 1998; Langmuir et al., 1999; Shuvaeva et al., 2000). This study considers arsenopyrite-rich mine waste that underwent 50a of oxidation.

The Arsenopyrite Residue Stockpile (ARS) is the product of the Nor-Acme Gold Mine, which operated in Snow Lake, Manitoba (Canada) from 1950 to 1959 (Fig. 1). The Nor-Acme Gold Mine is located in the Paleoproterozoic Flin Flon-Snow Lake volcano-sedimentary greenstone belt (Richardson and Ostry, 1996). Ore zones consist of quartz-carbonate veins containing free Au overgrowing sulfide minerals, and refractory Au inside the grains of sulfide (Richardson and Ostry, 1996). The ore assemblage is dominated by arsenopyrite with minor pyrrhotite, pyrite and chalcopyrite. Gangue minerals include quartz, albite, actinolite, calcite and biotite (Fulton, 1999).

^{*} Corresponding author.

E-mail address: ksalzsauler@golder.com (K.A. Salzsauler).

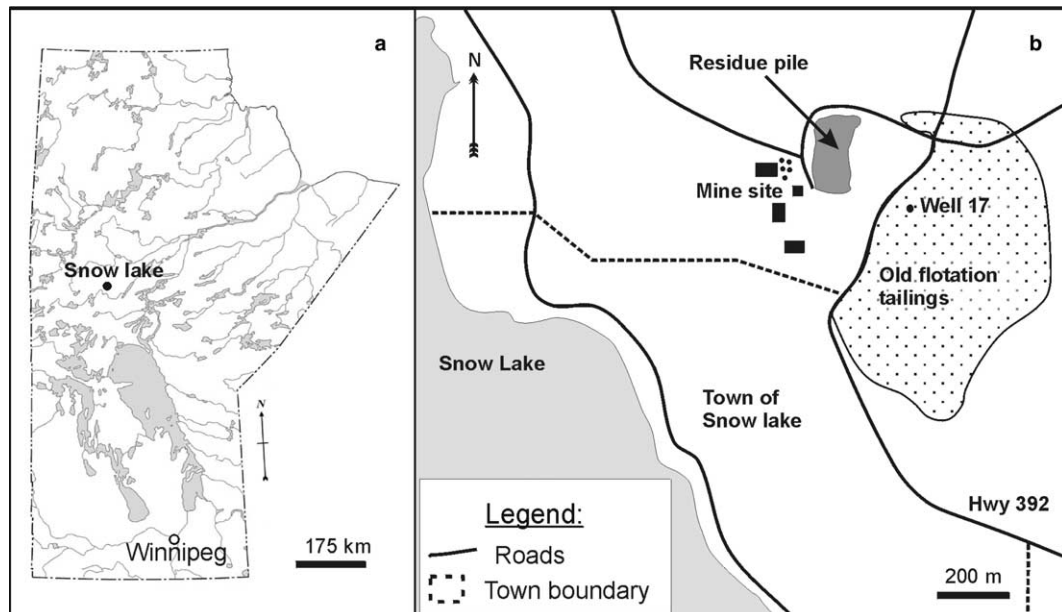


Fig. 1. (a) Location of Snow Lake, Manitoba. (b) The town of Snow Lake, showing the New Britannia Mine site, the arsenopyrite residue pile and the old Nor-Acme emergency flotation tailings.

Ore bearing sulfides were concentrated by flotation in the Nor-Acme mill. Flotation concentrates proceeded to a cyanidation circuit where accessible Au was dissolved (Convey et al., 1957). The Au-bearing fluids were filtered prior to transfer to precipitation units. Dewatering of the cyanidation fluids left a waste by-product of concentrated

sulfides still containing refractory Au. From 1950 to 1959, 250,000 ton of this residue, consisting of up to 60% sulfides, was piped into an uncapped waste rock impoundment measuring 182 m long, 85 m wide and 10 m high (Fig. 2). The average grade of this refractory waste material is 0.28 ounces of Au per ton, for a total of 2000 kg Au (Richardson



Fig. 2. The Nor-Acme Site, circa 1950. The Arsenopyrite Stockpile (A) was located north of the original mill, and the “emergency” flotation tailings (F) in a swamp to the east of the mill (Snow Lake Historical Records).

and Ostry, 1996). Despite several attempts, no economically viable, environmentally safe method has been identified to extract the Au and dispose of the As-rich waste that would be generated.

In 1995, the Nor-Acme mine reopened as the New Britannia Mine, with the ARS being designated as an orphaned site and the responsibility of the Crown. In 2000, a multilayer cap of waste rock and silt was placed on the pile by New Britannia Mine, to prevent water infiltration, and further oxidation of the wastes, and to reduce the flow of contaminated runoff (Sikamen, 1988). However, groundwater in a monitoring well south of the ARS still has concentrations of >20 mg/L As, which is 40 times greater than the Mining Metal Effluent Regulation for As release from active mine sites in Canada of 0.5 mg/L (MMER, 2003).

The objectives of this study were to investigate the geochemical behavior of As in the high sulfide mine wastes in the ARS, and to determine the source and reason for high As content in an adjacent groundwater plume. The objectives were achieved through identification of solid As phases, determination of As speciation in the pore water, and thermodynamic calculations.

2. Methodology

Solid samples were taken from the surface of the ARS by New Britannia Mine in 1998 (prior to the emplacement of the cap) and stored in a closed container at room temperature. In March 2002, four sampling holes were drilled into the ARS using a sonic drill (Fig. 3). Solid cores, 6.25 cm in diameter were extracted from depths of 8.6–14.6 m below ground surface. The core was frozen immediately after sampling in the −40 °C air temperature and transported frozen to prevent oxidation. The cores are different lengths due to the asymmetrical shape of the pile (Fig. 3).

In the laboratory, the core was split in half while still frozen and logged with respect to morphological variations and color determined with Munsell® soil color charts. Sections of core, measuring 15–20 cm in length, were removed from half of the core at approximately 1.5-m intervals, defrosted and air-dried at room temperature. These samples were analyzed by Activation Laboratories Ltd. (Actlabs) using a combination of induced neutron activation analysis (INAA) and aqua regia dissolution, followed by inductively coupled plasma (ICP) optical emission spectroscopy (OES) and mass spectroscopy

(MS) analysis. Sulfate, carbonate (CO₂), Cl, and F were analyzed using infrared, ISE and INAA analysis.

The mineral composition was determined using a combination of powder X-ray diffraction (XRD), μXRD, electron microprobe analysis (EMP) and scanning electron microscopy (SEM) with energy dispersive spectrometry (EDS), and polished thin sections were made in the absence of water to prevent dissolution of soluble phases. Powder XRD data were collected using a Phillips PW 1729 diffractometer with Ni-filtered Cu K α radiation generated at 40 kV and 40 mA, and 0.5° beam slit. Optically differentiated phases in thin sections were analyzed using a Bruker Discover μX-ray diffractometer operated with Cu K α radiation generated at 40 kV and 40 mA at the University of Western Ontario. The combination of a Gobel mirror parallel optics system and a general area detector system (GADDS) enabled in situ collection of data from polished thin sections (Flemming et al., 2005). The beam diameter could be collimated to 500, 300 or 50 μ m. Phases were identified using the ICDD database.

Polished thin sections were analyzed qualitatively using a Cambridge Instrument Stereoscan 120 SEM and quantitatively using a CAMECA-SX100 EMP at the University of Manitoba. The EMP was operated at an acceleration potential of 15 kV, a beam current of 15 nA measured on a Faraday cup with a 20- μ m beam diameter, and using the standards diopside (Si, Ca), arsenopyrite (Fe, As, S), chalcopyrite (Cu), gahnite (Pb, Zn), albite (Na), feldspar (K) and andalusite (Al). The raw data were corrected by the PAP correction procedure (Pouchou and Pichoir, 1985). Detection limits for different components varied from 0.01 to 0.05 wt%, and analytical precision was approximately 2% for most major elements, and 10% for minor elements.

Samples of frozen core samples were transported to Activation Laboratories Ltd in sealed coolers under ambient atmospheric conditions. Pore water was extracted from samples of core by Activation Laboratories Ltd. in a N₂ atmosphere to prevent changes in As speciation. These pore-water samples were passed through 0.2 μ m filters and divided into four aliquots. The aliquot for the analysis of dissolved metals was preserved with HNO₃, for Fe speciation with HCl, and the aliquots for As speciation and anion analysis left unacidified. Dissolved metals were measured by ICP-MS and ICP-OES, anions by ion chromatography and alkalinity by titration. Arsenic was separated into redox species using a

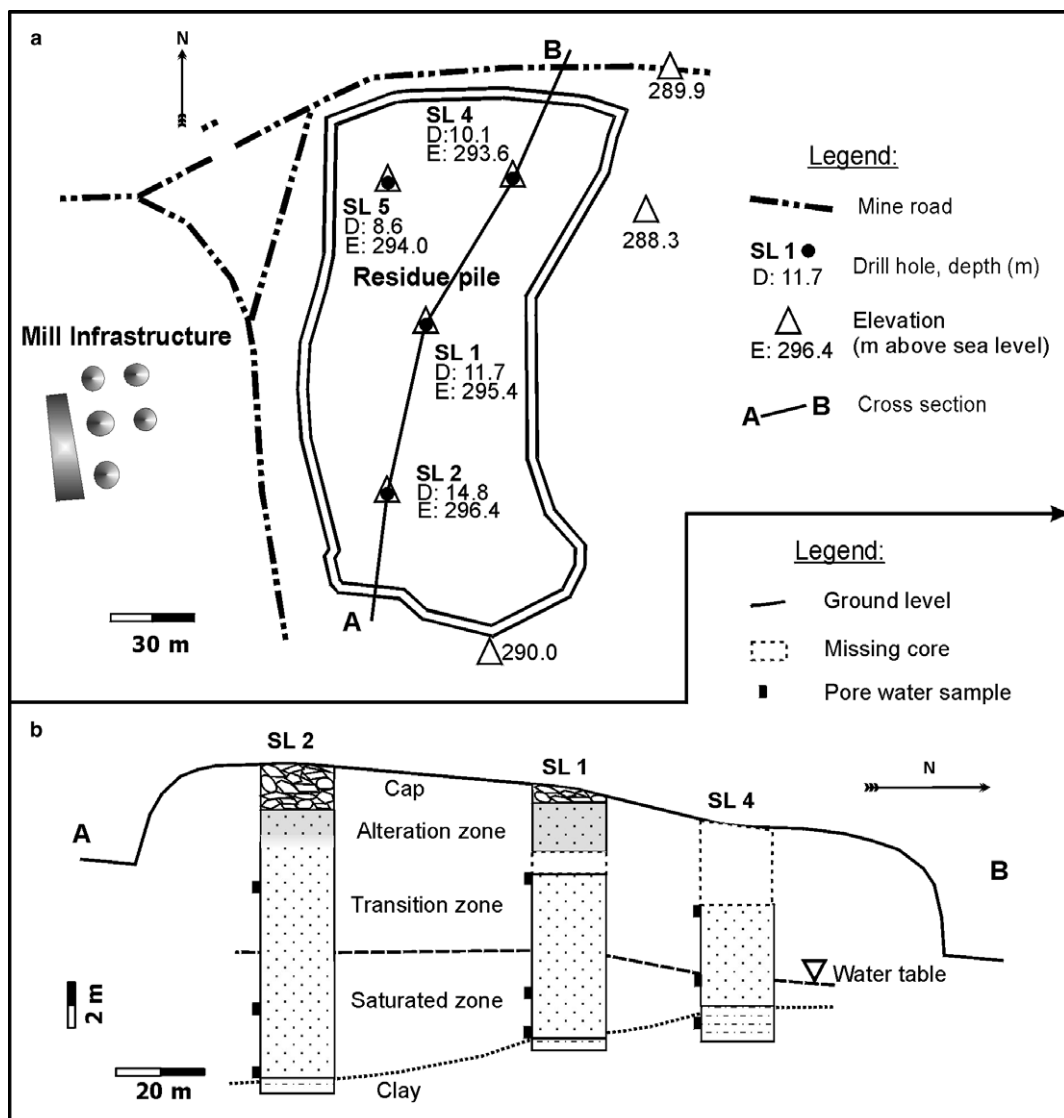


Fig. 3. (a) The elevation and location of drill holes in the ARS. (b) A schematic cross-section (AB) of the ARS from south (SL2) to north (SL4); not to scale.

P/ACE MDQ Capillary Electrophoretic System (Beckman Coulter) with a high resolution (HR) ICP-MS detector. Total Fe concentration was measured by HR-ICP-MS; concentration of Fe(II) was determined using a P/ACE MDQ Capillary Electrophoretic System (Beckman Coulter) with UV detection. Iron(III) concentration was calculated as the difference between total Fe and Fe(II).

Duplicate pore water samples were extracted at the University of Manitoba. Arsenic species were separated by passing filtered water through ACCU-BOND II Strong Anion Exchange (SAX) cartridges (Le et al., 2000) at a rate of 1 mL/min. The SAX

cartridge retained arsenate anions while arsenite passed through. The arsenite solution was acidified with concentrated HCl. The cartridge was then eluted with 10 mL of 1 M HCl to release the arsenate. Aliquots containing As(III), As(V), and total As were analyzed by ICP-OES at the University of Manitoba.

A charge balance of ions in solution and saturation indices (SI) of phases controlling water composition were assessed using the geochemical modeling program WATEQ4F (Ball and Nordstrom, 1991). Redox disequilibrium for Fe(II)/Fe(III) and As(III)/As(V) couples generally occurs in natural waters

(Lindberg and Runnels, 1984), therefore, these couples were decoupled in WATEQ4F input to calculate activities of Fe and As species.

3. Results

3.1. Morphology and composition

Although the pile rises to only 5 m above the ground surface, the total depth of residue extracted in the drill cores measured between 10.0 and 14.6 m (Fig. 3). The ground surface dips towards the north of the pile and hence the surface runoff drains to the NW. The pile is underlain by reddish-brown, silty clay. Although the base of the pile dips to the south, the direction of the local ground water flow has not yet been defined.

Primary, unoxidized sulfide residue extends from about 2 m below the top of the residue to the base of the pile (Fig. 3). The primary residue consists of very fine-grained (30–50 µm) arsenopyrite, pyrrhotite, pyrite and chalcopyrite (in order of decreasing abundance). Silicate minerals are predominantly quartz, albite, orthoclase, biotite and actinolite. Primary grains are anhedral to subhedral with smooth grain boundaries. Although no carbonate minerals were detected by XRD or SEM, bulk geochemical analysis suggests that up to 5.5 wt% calcite is present. In the altered wastes, primary phases occur as inclusions in secondary phases. *Unoxidized sulfide residue* contains up to 23 wt% As, 25 wt% Fe and 18 wt% S, with <17 ppm Au. Although disintegration of some pyrrhotite, pyrite and arsenopyrite grains was observed optically, no secondary solid phases were found in this material.

The altered part at the top of the pile can be divided into the *upper alteration zone* (0–10 cm), the *lower alteration zone* (10–40 cm) and the *transition zone* (40 cm to 2 m). *Highly altered material*, taken from the top of the pile prior to the emplacement of the cap, allowed the study of “end-member” oxidation products.

The *transition zone* represents a diffuse boundary between the oxidized and unoxidized material. It consists of friable, dark grayish brown (2.5Y4/2), very fine-grained (45 µm) arsenopyrite, pyrite, chalcopyrite and pyrrhotite. It is chemically and mineralogically similar to the unoxidized material, containing 17.4 wt% As, 22.5 wt% Fe and 16.0 wt% S, and <2.7 wt% CO₂ (equivalent to 6 wt% calcite). However, the transition zone is distinct from the *unoxidized sulfide residue* as it is mottled with

scorodite aggregates. Rare X-ray amorphous Fe sulfo-arsenates (AISA) and jarosite were found in small veins penetrating into the zone from upper horizons.

The *lower alteration zone* consists of a light brownish grey mixture (2.5Y6/2) of secondary alteration products with <30% altered sulfides, arsenopyrite, pyrite and chalcopyrite. The composition is <15.0 wt% As, 16.6 wt% Fe, 10.5 wt% S and 0.2 wt% CO₂ (equivalent to 0.5 wt% calcite). Secondary phases include scorodite, AISA and jarosite.

The *upper alteration zone* consists of layers of friable, light olive brown and yellow AISA (2.5Y7/8 and 2.5Y5/4, respectively) interbedded with layers of green-grey (5G5/2), slightly altered sulfides. Although this zone is chemically and mineralogically similar to the *lower alteration zone*, more oxidized material is found in the yellow-brown layers. Up to 15.9 wt% As, 17.9 wt% Fe and 8.8 wt% S are concentrated in the upper 10 cm of the pile. The secondary phases are AISA, scorodite and jarosite, with scorodite and remnant arsenopyrite, pyrite and chalcopyrite being concentrated in the green-grey layers.

In the *highly altered material*, the refractory residue consists of a hardened, gel-like dark yellowish brown (10YR3/4) AISA coating powdery, yellow (5Y7/6) to brownish yellow (10YR6/8) AISA and powdery, grayish green (5G5/2) Fe arsenates. It contains up to 12.9 wt% As, 13.2 wt% Fe and 6.9 wt% S. There is no pyrrhotite or chalcopyrite but trace amounts of arsenopyrite and pyrite occur as inclusions in secondary phases. The dominant secondary mineralogical phases in this material include AISA, scorodite and rare jarosite.

3.2. Secondary alteration products

Three groups of secondary phases contain As: AISA, scorodite and jarosite. Scorodite was identified in the *highly altered material* and in the alteration and transition zones by µXRD (Flemming et al., 2005).

The earliest secondary arsenate phases to form are 50 to 300 µm microcrystalline aggregates of scorodite which cement primary silicate and sulfide grains (Fig. 4). This is the major morphology of scorodite in the *transition* and the *upper alteration zones* and has an average composition of 34.6 wt% As, 0.6 wt% S and 24.7 wt% Fe. A second form of scorodite consists of anhedral, equant 5 µm grains, which are now enclosed in AISA cement (Fig. 5).

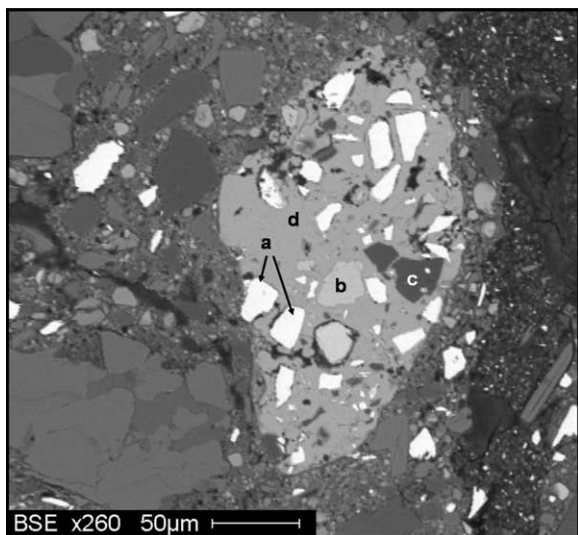


Fig. 4. SEM electron backscatter image of arsenopyrite (a), pyrite (b), and silicate (c) inclusions in a scorodite (d) aggregate in the transition zone of drill core SL2.

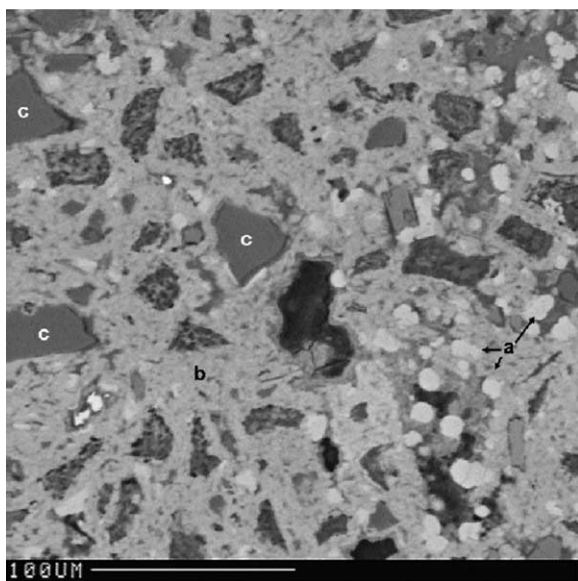


Fig. 5. SEM electron backscatter image of microcrystalline, ball-like scorodite inclusions (a), in an AISA matrix (b), and containing inclusions of primary silicates (c) in a sample of highly altered material.

They have an average composition of 35.2 wt% As, 1.0 wt% S and 26.0 wt% Fe (Table 1).

The dominant arsenopyrite alteration product is yellow-orange-brown gel-like AISA forming zoned spherules about 500 µm in diameter. The cores of these spherules contain a mixture of <60% primary silicate gangue, and altered sulfide grains cemented

by AISA(1) (Fig. 6). The spherules have thick rims of reddish-brown, homogeneous AISA(2) gel-like material up to 50 µm thick. Fragments of this homogeneous AISA(2) are also found in the alteration zone. The sequence of precipitation of AISA generations can be inferred by morphological relation of AISA phases (Fig. 7). The earlier AISA have higher As/S ratios than later forming AISA(2). AISA(1) cement is compositionally close to zýkaite ($\text{Fe}_4\text{-}(\text{AsO}_4)_3(\text{SO}_4)(\text{OH}) \cdot 15\text{H}_2\text{O}$), an alteration product of arsenopyrite that is found in association with scorodite and pittcrite (Anthony et al., 2000). Physical and chemical characteristics of AISA(2) are comparable to pittcrite, which has been retained as a generic name for amorphous gel-like Fe(III) arsenate with no apparent stoichiometry (Dunn, 1982; Dunn et al., 1983; Anthony et al., 2000).

There are two distinct compositions of potassio-hydronium jarosite. Low-As-jarosite (<0.6 wt% As) forms very fine grained inclusions in AISA(2) in the *upper alteration zone* and the *highly altered waste*. High-As-jarosite (0.6–5.8 wt% As) occurs in the *lower alteration zone* as anhedral inclusions (20–50 µm in diameter) coated by rims of AISA(2) (Fig. 8).

3.3. Chemistry of pore water

Cores SL4, SL1 and SL2, which transect the pile from NW to SE (Fig. 3) were selected for pore water extraction. Water could only be extracted below about 4 m depth because the core was too dry above this level. The regions selected for pore water extraction were the base of the pile, a region about 2 m above the base where the core was saturated with water, and the transition layer about 4 m from the top of the residue.

Pore water had a pH of 6.7–8.6, and contained up to 7420 mg/L SO_4 . The lowest values of pH and the highest SO_4 , Fe, K, Ca and Mg contents were in the drier transition zones (Table 2). Iron(II) dominated over Fe(III) in all samples.

Comparison of the results of As speciation in the pore waters obtained by two different techniques demonstrates that the levels of concentration in the same samples and the pattern of the species distribution are reproducible (Table 2). In the *transition zone* concentrations of total As are lower on average than for samples from the saturated zone or the base of the pile. The total As concentrations are higher in cores SL2 and SL4 (located in the NE and SW quadrants of the pile) than in SL1 (from the

Table 1
Composition of secondary phases in the Arsenopyrite Stockpile (wt%)

Phase	Formula	Fe	As	S	K	<i>n</i> ^a
Scorodite (1) ^b	$\text{Fe}_{0.92}(\text{As}_{0.96}, \text{S}_{0.04})\text{O}_4 \cdot 2\text{H}_2\text{O}$	24.7	34.6	0.58	0.02	45
Scorodite (2) ^b	$\text{Fe}_{0.92}(\text{As}_{0.93}\text{S}_{0.06})\text{O}_4 \cdot 2\text{H}_2\text{O}$	26	35.2	1.02	0.01	12
Low As Jarosite ^b	$(\text{K}_{0.65}\text{H}_3\text{O}_{0.35}^+)_{\text{Fe}_{3.14}}(\text{S}_{0.98}\text{As}_{0.02}\text{O}_4)_2(\text{OH})_6$	32.0	0.62	11.4	4.6	2
High As Jarosite ^b	$(\text{K}_{0.7}\text{H}_3\text{O}_{0.3}^+)_{\text{Fe}_{3.07}}(\text{S}_{0.73}\text{As}_{0.2}\text{O}_4)_2(\text{OH})_6$	31.6	5.6	8.7	5.0	17
AISA(1) ^c		27.1	26.7	2.7	0.04	98
AISA(2) ^c		21.4	22.7	9.5	0.15	7

^a Total number of grains analyzed with similar geochemical, morphological and mineralogical characteristics.

^b Formulae and percentages for representative grains from the ARS.

^c AISA composition presented as an average of representative analyses.

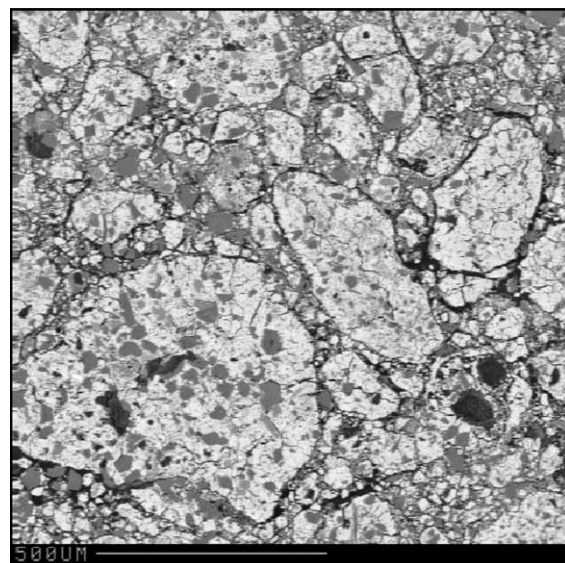


Fig. 6. SEM electron backscatter image of AISA “balls” in the upper alteration zone.

middle of the ARS). In all of the samples from the saturated zone and from the base of SL2, arsenate ion species dominated. Arsenite concentration was greater than arsenate in samples from the transition zone and from the base of SL1 and SL4.

A diagram of H–O–As–Fe–S was built in Eh–pH space with the “Act2” program available in the “Geochemist’s Workbench” package, using the LLNL database (Bethke, 1996). Activities of arsenate, Fe(II) and SO₄ were taken close to their average molar concentrations in pore waters of 10⁻³, 10⁻⁴ and 10⁻², respectively. Under these conditions, the only stable phase on the Eh–pH diagram is goethite, which was not detected in any ARS samples. As the solubility product of scorodite varies from 10⁻²⁰ to 10⁻²⁴ depending on the crystallinity of the phase (Krause and Ettel, 1988), the solubility product in LLNL database (10^{-20.2}) was replaced

with the lower *K*_{sp} (10^{-24.4}) reported by Krause and Ettel (1988). In this case, scorodite appears on the diagram where the pH is less than 3.84 (Fig. 9(a)). However, according to this plot, scorodite could not be formed as a stable phase from the high pH of the pore solutions found in the ARS. If goethite precipitation is suppressed from this system (Fig. 9(b)), the field of scorodite stability extends to pH 7.27, where it is in equilibrium with amorphous Fe(OH)₃. The pore water samples from the transition zone now plot in the scorodite field, indicating that this mineral could precipitate as a metastable phase.

Saturation indices (SI) were calculated using thermodynamic constants in WATEQ4f and data from Table 2, including the As values obtained by Actlabs. Where saturation indices are <0, the mineral should dissolve in solution (undersaturated), and if >0, the mineral is thermodynamically stable or can be precipitated from solution (oversaturated) (Ball and Nordstrom, 1991). Average values indicated that gypsum (SI = 0.0), calcite (SI = 1.0), dolomite (SI = 0.6) and siderite (SI = 0.3) were in equilibrium with the pore water. They also showed that jarosite solid solution (SI = -3.5) and scorodite (SI = -4) would be unlikely to precipitate from the present pore solutions. It should be noted that these saturation indices were calculated using thermodynamic constants that may vary depending on the composition of jarosite and the crystallinity of scorodite (Alpers et al., 1989; Krause and Ettel, 1988). If the lowest value for scorodite solubility is used in the calculation, the solutions will be saturated with respect to scorodite. Arsenic phases, such as arsenolite, arsensiderite, mansfieldite and As₂O₅ have SI < -5 and would be even less likely to precipitate than scorodite.

A sample of water from Monitoring Well 17, 200 m SE of the ARS, had a pH of 6.39, 2180 mg/L SO₄²⁻, 24 mg/L Fe²⁺, 38 mg/L Fe³⁺, 17.8 mg/L

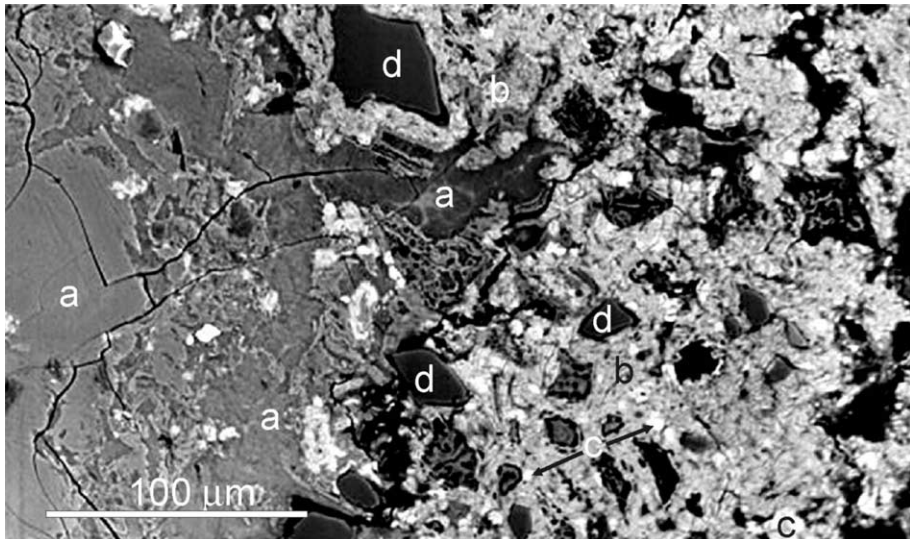


Fig. 7. SEM electron backscatter image showing the relationship between scorodite and varieties of AISA in the *highly altered material*. AISA(2) (a) coats AISA(1) (b), which contains inclusions of scorodite (c), and resistant silicate grains (d).

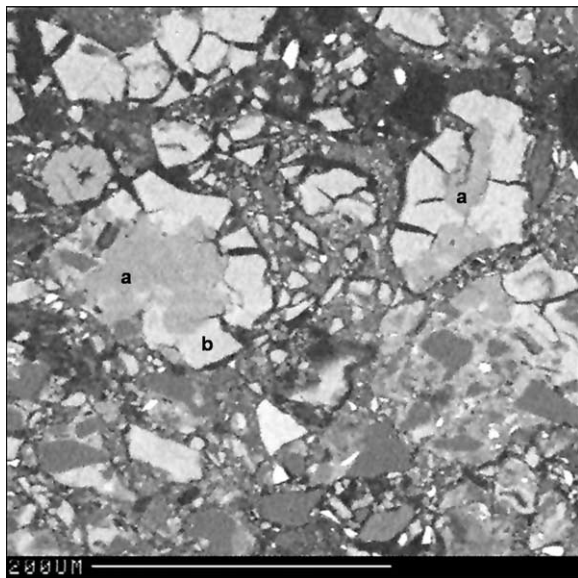


Fig. 8. SEM electron backscatter image of high As jarosite (a), coated with a thin rim of AISA (b), in a mélange of altered refractory sulfide material and AISA fragments in the *lower alteration zone*.

As^{3+} and 1.7 mg/L As^{5+} . A reddish brown precipitate formed in a filtered unacidified aliquot of this water after being stored for two months. These sediments can give direct information about the phases that might precipitate from the water during the oxidation of Fe(II) (Sidenko and Sherriff, 2005). SEM-EDS analysis showed the Snow Lake precipitate to

consist of spherules, 2 μm in diameter, containing Fe and As. The material gave an XRD pattern similar to poorly crystalline, 2-line ferrihydrite.

4. Discussion

The source of As in the ARS is primary, refractory (Au-bearing) arsenopyrite. Although pyrrhotite is the most susceptible sulfide phase to oxidation (Jambor, 2003), arsenopyrite, as the major sulfide mineral in the ARS, is the dominant source of SO_4 , Fe and As in ARS pore water. Arsenopyrite is stable in low Eh, high pH conditions in the unoxidized residue. At depth, pyrrhotite is the only sulfide mineral to show initial stages of dissolution. In the *lower alteration zone*, pyrrhotite has been completely altered but arsenopyrite, pyrite and chalcopyrite are still present as inclusions in secondary phases. Only trace amounts of arsenopyrite and pyrite have survived, as inclusions in secondary phases, in the *highly altered material* collected from the surface of the pile.

Oxidation would have been initiated during deposition of the residue and continued for 50a prior to the emplacement of the cap (Plumlee, 1999). The first products of arsenopyrite oxidation are Fe(II) and As(III)

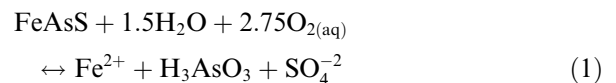


Table 2
Composition of pore water squeezed from the ARS core (mg/L)

	Transition zone			Saturated zone			Base			LOD
	SL2	SL1	SL4	SL2	SL1	SL4	SL2	SL1	SL4	
Depth (m)	5	4	4	11	9	7	14	11	9	
pH	7.9	6.7	7.3	8.6	8.3	7.9	8.3	7.8	8	
Eh _{NHE} (mV)	78	81	79	36	51	157	72	100	84	
Total As ^a	4.9	10.5	21.2	100.2	27.2	63.4	91.4	11.4	36	0.00003
As(III) ^a	9.7	—	13.5	13.2	6.6	3.4	13.2	11	24.5	0.01
As(V) ^a	2.4	—	0.7	67	16.5	46.5	70.1	0.5	3.8	0.01
Total As ^b	5.8	6.4	16.5	20.7	10.2	62.9	77.6	15.7	28.6	
As(III) ^b	12.5	8.5	14.8	4.6	6.3	28.9	35.9	7.5	18.8	
As(V) ^b	1.3	0.8	8.8	17.9	8.3	38.1	51.7	17.1	5.7	
Total Fe ^a	0.4	917.3	23.8	5.7	3	2.5	4.7	2.4	1.6	0.005
Fe(II) ^a	0.5	915	10.9	1.7	2.4	1.7	1	1.6	1	0.01
Fe(III) ^a	0.3	6.8	1.2	1	0.4	0.6	0.3	0.4	0.3	0.01
Al	0.2	3.8	0.3	0.4	0.4	0.7	1.3	0.4	0.4	0.002
B	2	1.1	2.6	0.1	0.1	1	0.1	0.1	0.5	0.001
Ba	0.1	—	0.2	0.1	0.1	0.1	0.1	110.2	0.1	0.0001
Ca	537	674	614	187	642	644	482	571	605	0.05
Cl	6.4	93.7	6.9	10.1	11.3	10.3	17.6	15.3	3.8	0.0005
F	4.5	<0.4	1.5	2	2.4	3.4	2.8	3.3	1.6	0.0005
HCO ₃ ⁻	—	—	158	167	63	133	222	—	135	
K	172	91	134	80	64	40	30	24	9	0.01
Mg	1030	1350	702	3	14	45	25	176	112	0.001
Mn	0.1	18.9	1.9	0	0	0	0.1	177	0.6	0.0001
Na	28.2	53.1	91.7	670	209	239	507	479	336	0.005
NO ₃	0.5	1.6	0.2	3.3	0.3	0.4	0.7	0.4	0.2	0.0005
Si	1.6	4.9	5.6	8.1	2.4	4.5	7.3	5.3	5	0.05
SO ₄	4770	7420	4240	1590	1910	1870	1710	2190	2140	0.001
Charge balance (%)	−10	−8	−7	−33	−14	−18	−29	−34	−19	

LOD = Limit of detection.

Note. Charge balance calculated with analytical total As and total Fe concentrations.

^a Values from Activation Laboratories.

^b Values from the University of Manitoba.

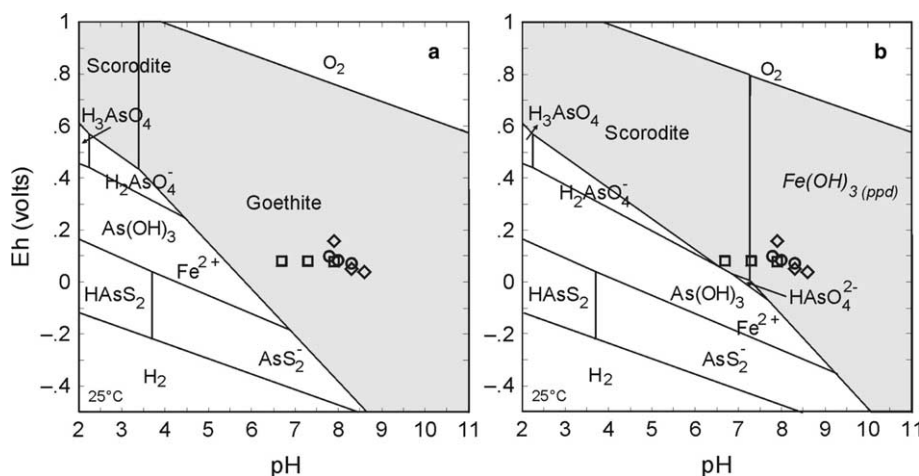
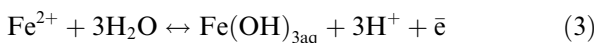
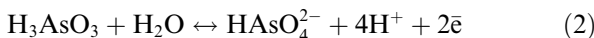


Fig. 9. Diagram of H–O–As–Fe–S built in Eh–pH space showing the scorodite field of stability (a) with respect to goethite and (b) to amorphous Fe(OH)₃. Activities of arsenate, Fe(II) and SO₄ were 10⁻³, 10⁻⁴, and 10⁻², respectively. Pore water compositions are indicated by squares for the transition zones, diamonds for the saturated zone and circles for the base of the pile.

After release into solution, Fe(II) and As(III) are oxidized by reactions 2 and 3 (assuming species that dominate at near-neutral pH in solution).

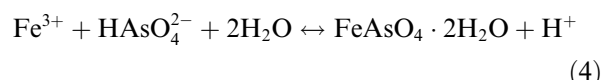


Pore water samples with a low pH have a high measured As(III):As(V) ratio because they are close to the As(III)/As(V) redox boundary (Fig. 9(b)). Samples with a higher pH are scattered in the field of As(V) further from the equilibrium boundary. The relationship between As speciation and pH was examined by correlating the ratio of As(III) to As(V) with pH and Eh. A negative correlation was found between the ratio of As(III):As(V) and pH. The correlation coefficients of -0.75 for the values from Activation Laboratories Ltd and -0.65 for those obtained at the University of Manitoba are statistically significant at the 95% probability level, despite the small range of pH values from 6.7 to 8.6. These correlations indicate that a lower pH favors the As(III) redox state.

The equilibrium Eh for As and Fe species was calculated to identify which redox couple is controlling the measured Eh in the pore waters. The equilibrium Eh was calculated from reactions 2 and 3. The calculated redox potential for the Fe species is slightly higher than the measured Eh in the saturated zone and at the base of the pile and much higher in the transition zone (Table 3). In contrast to Fe, the measured Eh equilibrium redox potential for As is significantly lower than the measured Eh due to the possible kinetic disequilibrium between As(III)/As(V) (Lindberg and Runnels, 1984). Therefore, the measured Eh is between the values calculated for both redox couples and closer to the redox potential of the Fe species, indicating that the Fe(II)/Fe(III) couple is the dominant couple controlling the measured Eh. However, As species

modify the bulk Eh somewhat by reducing it with respect to the equilibrium potential of the Fe species.

The earliest stages of precipitation of secondary As phases appear to be preserved in the *transition zone*. Here, scorodite occurs as discrete, ball-like aggregates, cementing moderately altered arsenopyrite grains. The enclosure of arsenopyrite would have reduced the probability of further oxidation. In the uncapped pile, the reaction of arsenate and Fe^{3+} ions in the pore water causes the precipitation of scorodite



According to the Eh–pH diagram (Fig. 9(b)), scorodite could precipitate as a metastable phase from near neutral pore solutions of the *transition zone* even after capping.

Acid produced during the oxidation of sulfides and precipitation of scorodite (reactions (1) and (4)) was initially buffered by the dissolution of the carbonate phases detected by chemical analysis (e.g. calcite)



With the advancement of sulfide oxidation and the dissolution of available neutralizing phases in the upper zones of the ARS, the pH of pore water would have been reduced. Prior to the emplacement of the cap, the surface water on the pile had a pH of 3.6 and the runoff a pH of 3.0 (UMA, 1987). Under these conditions, scorodite becomes stable with respect to goethite (Fig. 9(a)).

Jarosite-group minerals can precipitate at low pH (<3) in the presence of high concentrations of $\text{Fe}(\text{III})$ and SO_4 (Baron and Palmer, 1996; Dutrizac and Jambor, 2000). In the pH conditions measured in the *transition zone* pore water, jarosite should not

Table 3
Measured and calculated redox potential of ARS pore water (mV)

	Transition zone			Saturated zone			Base		
	SL2	SL1	SL4	SL2	SL1	SL4	SL2	SL1	SL4
Depth (m)	5	4	4	11	9	7	14	11	9
Eh _{measured}	78	81	79	36	51	157	72	100	84
Fe(II)/Fe(III)	186	286	249	61	82	172	97	181	150
As(III) ^a /As(V) ^a	-211	-	-160	-255	-228	-159	-219	-221	-229
As(III) ^b /As(V) ^b	-222	-	-128	-258	-237	-189	-235	-170	-220

^a Values from Activation Laboratories.

^b Values from the University of Manitoba.

be capable of precipitating. However, the occurrence of jarosite and AISA in small veins indicates that they might precipitate from solutions percolating from the upper horizons, where the conditions of pH could have been lower prior to capping.

Jarosite can incorporate AsO_4^{3-} by the partial replacement of SO_4^{2-} in the unit cell (Dutrizac et al., 1987; Paktunc and Dutrizac, 2003; Savage et al., 2005). In the ARS, jarosite contains up to 5.8 wt% As with that from the *highly altered material* having a lower As concentration than from the *alteration zone*. Dutrizac et al. (1987) found that the concentration of As incorporated into synthetic jarosite decreased at low pH, with a corresponding increase in Fe and SO_4 . Sequential extraction showed that <1 wt% of the bulk sample consists of jarosite in the *upper alteration zone* (Salzsauler, 2004). Therefore, jarosite may have only a minor role in removing As from solution.

The precipitation of low-solubility, thermodynamically favored, crystalline scorodite and jarosite is followed by the precipitation of disordered, more soluble phases such as AISA. X-ray amorphous Fe sulfo-arsenates (AISA) appear to have been the final phase forming from late stage, high As and Fe solutions. Compositionally similar X-ray amorphous material was described by Gieré et al. (2003) in sulfide waste from a Au mine. Very fine-grained scorodite (2) inclusions, found in AISA(1) from the *highly altered material*, must have formed prior to AISA. They may represent the remnants of scorodite (1) aggregates that partially dissolved in acidic conditions. However, a wide range of arsenic (28.8 to 37.5 wt%) and iron (24.8 to 27.2 wt%) in scorodite (2) inclusions in the *highly altered material* suggests that this mineral is distinct from scorodite (1) aggregates in the *alteration zone* and has been formed later.

Pittcite (AISA(2)), the final product to form, is a dehydrated gel coating aggregates of AISA(1). Although the *alteration zone* was too dry to extract water for analysis, similar conditions were observed by Sidenko et al. (2001) in high sulfide mine wastes in Siberia, where AISA type phases precipitated from pore water characterized by high SO_4 (180 g/L), As (22 g/L) and Fe (57 g/L) concentrations, and low pH (1.7).

With the addition of the waste rock cap, the source of atmospheric O_2 that fueled the precipitation of secondary As phases has been removed. Existing phases such as jarosite, scorodite and AISA are unstable in the present conditions of the pore

water in the ARS, and theoretically could be recrystallized as goethite (Fig. 9(a)). Now, the concentrations of As, Fe and SO_4 in the pore water of the capped pile are controlled by the dissolution of residual arsenopyrite grains and unstable secondary phases, which depend on the pH and redox state of the system. Arsenic released from these phases could be only partially adsorbed by Fe oxyhydroxides stable in the present conditions of pore waters. A combination of these effects may explain the high level of As in pore water towards the base of the residue, which is up to 20 times higher than in the transition zone.

5. Conclusion

This study traced the passage of As in high sulfide, arsenopyrite mine waste stored for over 50a because of its potentially valuable refractory Au. Oxidation of arsenopyrite, the primary source of As, occurred during deposition and for 50a of exposure to the atmosphere. This resulted in the precipitation of As in the form of secondary scorodite, jarosite, and amorphous Fe sulfo-arsenate at the top of the pile and a lowering of pH. Covering the pile with a clay and waste rock cap prevented further oxidation and generation of acid. Arsenic, released during the previous oxidative phase or now from gradual breakdown of arsenopyrite, continues to seep into the groundwater possibly causing the high values in a monitoring well SE of the ARS. Thermodynamic calculations show that Fe oxyhydroxides may precipitate, and partially remove As from solution by adsorption.

Further work is in progress to investigate the reactions occurring in the orphaned tailings SE of the ARS. The direction and rate of flow of the groundwater in the vicinity of the ARS and the orphaned tailings will also be determined.

Acknowledgments

This study was supported by funding from Manitoba Industry, Economic Development and Mines, and an NSERC discovery Grant to B.L.S. Dr. R. Flemming (University of Western Ontario) provided access to the μXRD . We thank Sergio Meija, Neil Ball, Ron Chapman and Gregg Morden for technical support at the University of Manitoba and Jennifer Kavalech for her assistance with field sampling. We appreciate the comments of Dr. Logsdon on thermodynamic modeling. We thank

Dr. Donald Langmuir, Dr. Richard Wanty and an anonymous reviewer for comments on this manuscript.

References

- Alpers, C.N., Nordstrom, D.K., Ball, J.W., 1989. Solubility of jarosite solid solutions precipitated from acid mine waters, Iron Mountain, California, USA. *Sci. Geol., Bull.* 42, 218–298.
- Anthony, J., Bideaux, R., Bladh, K., Nichols, M., 2000. Handbook of Mineralogy Arsenates, Phosphates, Vanadates, vol. IV. Mineral Data Publishing, Tuscon, AZ.
- Ball, J.W., Nordstrom, D.K., 1991. User's manual for WATEQ4f, with revised thermodynamic database and test cases for calculating speciation of major, trace, and redox elements in natural waters. US. Geol. Surv. Open-File Rep. #91-183.
- Baron, D., Palmer, C., 1996. Solubility of jarosite at 4–35 °C. *Geochim. Cosmochim. Acta* 60, 185–195.
- Bethke, C.M., 1996. Geochemical Reaction Modeling. Oxford University Press, New York, p. 397.
- Convey, J., McLachlan, G., Carter, J., Wright, H., Banks, H., Airey, H., 1957. The milling of Canadian Ores. In: 6th Commonwealth, Mining and Metallurgical Congress.
- Dunn, P., 1982. New data for pittcite and a second occurrence of yukonite at Sterling Hill, New Jersey. *Mineral. Mag.* 46, 261–264.
- Dunn, P., Fleischer, M., Burns, R., Pabst, A., 1983. New mineral names. *Am. Mineral.* 68, 471–475.
- Dutrizac, J., Jambor, J., 2000. Jarosites and their application in hydrometallurgy. In: Alpers, C., Jambor, J., Nordstrom, D.K. (Eds.), Sulfate Minerals: Crystallography, Geochemistry and Environmental Significance. *Rev. Mineral. Geochim.* 40, 405–443.
- Dutrizac, J., Jambor, J., Chen, T., 1987. The behavior of arsenic during jarosite precipitation: reactions at 150 °C and the mechanism of arsenic precipitation. *Can. Metall. Quart.* 26, 103–115.
- Flemming, R.L., Salzsauler, K.A., Sherriff, B.L., Sidenko, N.V., in press. Identification of scorodite in fine-grained, high-sulfide, arsenopyrite mine waste using Micro X-ray diffraction (μ XRD). *Can. Mineral.*
- Fulton, P., 1999. Distribution of gold mineralization at the New Britannia Mine in Snow Lake Manitoba: Implications for exploration and processing. M.Sc thesis, Univ. Manitoba.
- Gieré, R., Sidenko, N.V., Lazareva, E.V., 2003. The role of secondary minerals in controlling the migration of arsenic and metals from high-sulfide waste (Berikul gold mine, Siberia). *Appl. Geochem.* 18, 1347–1359.
- Jambor, J., 2003. Mine waste mineralogy and mineralogical perspectives of Acid-Base Accounting. In: Jambor, J.L., Blowes, D.W. (Eds.) Environmental Aspects of Mine Wastes. Mineralogical Association of Canada Short Course 31, pp. 117–146.
- Krause, E., Ettel, V.A., 1988. Solubility and stability of scorodite, $\text{FeAsO}_4 \cdot 2\text{H}_2\text{O}$: new data and further discussion. *Am. Mineral.* 73, 850–854.
- Langmuir, D., Mahoney, J., MacDonald, A., Rowson, J., 1999. Predicting arsenic concentrations in the pore waters of buried uranium mill tailings. *Geochim. Cosmochim. Acta* 63, 3379–3394.
- Le, X.C., Yalcin, S., Ma, M., 2000. Speciation of sub microgram per liter levels of arsenic in water: On-site species separation integrated with sample collection. *Environ. Sci. Technol.* 34, 2342–2347.
- Leblanc, M., Achard, B., Ben Othman, D., Bertrand-Sarfati, J., Personné, J.Ch., 1996. Accumulation of arsenic from mine waters by ferruginous bacterial accretions (stromatolites). *Appl. Geochem.* 11, 541–554.
- Lindberg, R.D., Runnels, D.D., 1984. Groundwater redox reactions: an analysis of equilibrium state applied to Eh measurements and geochemical modeling. *Science* 225, 925–927.
- MMER (Mining metal effluent regulations) (April 30). <http://laws.justice.gc.ca/F-14/SOR-2002-222/text.html>. 2003 (Accessed November 22, 2003).
- Paktunc, D., Dutrizac, J., 2003. Characterization of arsenate for sulfate substitution in synthetic jarosite using X-ray diffraction and X-ray absorption spectroscopy. *Can. Mineral.* 41, 905–919.
- Plumlee, G., 1999. The environmental geology of mineral deposits. In: Plumlee, G., Lodgson, M. (Eds.) SEG Reviews in Economic Geology 6A: The Environmental Geochemistry of Mineral Deposits. pp. 70–116.
- Pouchou, J.L., Pichoir, F., 1985. “PAP” (phi-rho-Z) procedure for improved quantitative microanalysis. In: Armstrong, J.T. (Ed.), Microbeam Analysis. San Francisco Press, San Francisco, pp. 104–106.
- Richardson, D., Ostry, G., 1996. Gold deposits of Manitoba. Manitoba Energy and Mines, Geological Services, Economic Geology Report ER86 – 1 (2nd ed.).
- Roussel, Ch., Bril, H., Fernandez, A., 1998. Hydrogeochemical survey and mobility of As and heavy metals on the site of a former gold mine (Saint-Yrieix mining district, France). *Hydrogéologie* 1, 3–12.
- Salzsauler, K.A., 2004. A mineralogical and geochemical study of arsenic in alteration products of sulfide-rich, arsenopyrite bearing mine waste, Snow lake, Manitoba, M.Sc. Thesis, Univ. Manitoba.
- Savage, K., Bird, D.K., O'day, P.A., 2005. Arsenic speciation in synthetic jarosite. *Chem. Geol.* 215, 472–498.
- Shubaeva, O.V., Bortnikova, S.B., Korda, T.M., Lazareva, E.V., 2000. Arsenic speciation in a contaminated gold processing tailings dam. *Geostand. Newslett.* 24, 247–252.
- Sidenko, N.V., Sherriff, B.L., 2005. The attenuation of Ni, Zn, Cu, by secondary Fe phases from surface and ground water of two sulfide mine tailings in Manitoba, Canada. *Appl. Geochem.* 20, 1180–1194.
- Sidenko, N., Lazareva, E., Kolmogorov, Y., 2001. Coprecipitation of As, Zn, Cu and Pb with secondary iron minerals in the high-sulfide mine waste, Berikul mine, Russia. In: Cidu, R. (Ed.), Water-Rock Interaction-10, Sardinia, Italy, 10–15 June, 1281–1284.
- Sikamen Resources, 1988. Snow Lake Gold Project – Project Description and Environmental Assessment, Toronto, Ontario. Unpublished report.
- UMA Engineering Ltd. 1987. Snow Lake Corporation: Snow Lake Bioleach Project; Environmental Impact Statement.